Supplement of Atmos. Meas. Tech., 16, 5659–5679, 2023
https://doi.org/10.5194/amt-16-5659-2023-supplement

Atmospheric Measurement Techniques
Open Access

Supplement of

Quality evaluation for measurements of wind field and turbulent fluxes from a UAV-based eddy covariance system

Yibo Sun et al.

Correspondence to: Bilige Sude (sude@craes.org.cn) and Shaomin Liu (smliu@bnu.edu.cn)

The intention of this supplement is to guide the readers through the relevant equations about calculation of geo-referenced wind, turbulent fluxes as well as their measurement uncertainties, and to provide the procedures in calibration the mounting misalignment using the measured data from ‘box’ flight maneuver. Part A provides the formulas necessary to compute the geo-referenced 3D wind vector and their measurement error. Part B gives the detailed equations to calculate the fluxes of sensible heat, latent heat, carbon dioxide (CO_2), and the method to quantify the measurement uncertainty in them due to instrument noise. Part C provides the procedure and results for calibrating the mounting misalignment based on ‘box’ flight maneuver. References to the literatures are given at the end of this supplement.

1 Part A: Detailed equations for calculating the geo-referenced wind vector and measurement precision

Wind measurement by aircraft is challenging. The wind measurement components of the UAV-based EC system consist of sensors that measure air pressure (static and dynamic pressure), air temperature, and aircraft attitude, position, velocity, and angular velocity. From these measurements, two velocity vectors U_a (velocity of the air with respect to the aircraft) and U_p (velocity of the aircraft with respect to the Earth) are derived. The velocity of wind with respect to earth (i.e., geo-referenced wind vector) is the result of adding these two vectors together, as:

$$U = U_a + U_p \qquad (S1)$$

For our developed UAV-based EC system, this text provides the detailed formulas necessary to compute the geo-referenced wind vector. Approaches to compute the geo-referenced wind vector based on the combination of a multi-hole probe and navigation system are often similar in principle (Crawford and Dobosy, 1992; Williams and Marcotte, 2000; Khelif et al., 1999; Metzger et al., 2011). Figure S1 illustrates the transformational relation for calculating the geo-referenced wind vector by the current UAV-based EC system.

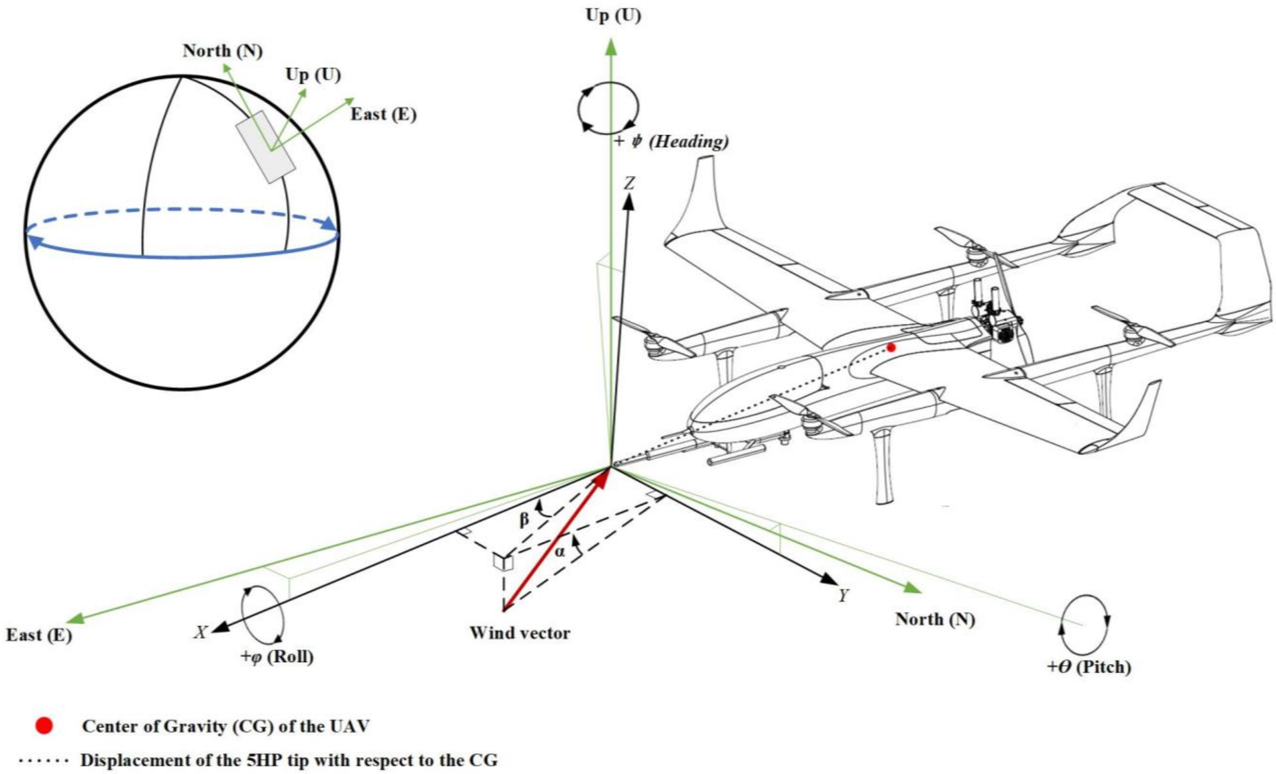

Figure S1. Diagram of the coordinate transformational relation for calculating geo-referenced wind vector. The green coordinate represents the geo-referenced coordinate system. The black coordinate represents the aircraft coordinate system.

Two coordinate systems are involved in calculating the geo-referenced wind vector: aircraft coordinate system (black in Fig. S1, *X*, positive forward, *Y*, to port, and *Z*, toward the airplane's roof) and geographic coordinate system (green in Fig. S1, *E*, positive eastward, *N*, northward, and *U*, upward). A transformation matrix, which is defined by measurements of the three conventional attitude angles: roll (φ), pitch (θ), and heading (ψ), accomplished rotation from the aircraft to the geographic coordinate. They must be applied in the following order: roll, pitch, and heading to convert from aircraft coordinate to geographic coordinate, and heading, pitch, and roll to convert the other way. The probe does not have to be located at the origin of the aircraft coordinate system. Based on the basic aircraft kinematics and the wind calculation equation given by Lenschow (1986), considering the influence of tangential velocity of rotation on the probe tip, the full expression to compute the geo-referenced wind vector can be expressed as:

$$U(t) = G(t)\widehat{U}_a(t) + U_p(t) + \Omega_p(t) \times R_p \quad \text{(S2)}$$

The unadorned symbols in Eq. (S2) are in geographic coordinate. The aircraft's coordinate is denoted by ("^"). G is the transformation matrix. Ω_p is the angular rate of the aircraft. The relative wind vector $\widehat{U}_a$ are measured by the five-hole probe (5HP) mounted on the nose of the UAV, usually extended on the forward part of the aircraft to reduce the measurable effects of the airflow distortion by the wing. The components of G, U_p and Ω_p are obtained from the integrated navigation system

(INS) outputs, which originate from the center of gravity (CG) of the UAV. U_p contains three velocity components toward east (u_p), west (v_p), and upward (w_p). R_p is the vector distance from the CG of the UAV to the 5HP tip.

The rotation matrix G from airplane to earth coordinates is computed in factored form by sequentially removing the dependence of the observed data on roll, pitch, and heading together with a relabeling of axes. The first rotation $T_1(\varphi)$ removes roll: it is a rotation about the X-axes with matrix representation:

$$T_1(\varphi) = \begin{bmatrix} 1 & 0 & 0 \\ 0 & cos\varphi & -sin\varphi \\ 0 & sin\varphi & cos\varphi \end{bmatrix} \tag{S3}$$

The next rotation $T_2(\theta)$ removes pitch:

$$T_2(\theta) = \begin{bmatrix} cos\theta & 0 & sin\theta \\ 0 & 1 & 0 \\ -sin\theta & 0 & cos\theta \end{bmatrix} \tag{S4}$$

The last rotation $T_3(\psi)$ removes heading:

$$T_3(\psi) = \begin{bmatrix} cos\psi & -sin\psi & 0 \\ sin\psi & cos\psi & 0 \\ 0 & 0 & 1 \end{bmatrix} \tag{S5}$$

The present coordinates of the hypothetical aircraft frame point north, east, and down, and must be transformed to east, north and up. This is done with the permutation T_4:

$$T_4 = \begin{bmatrix} 0 & 1 & 0 \\ 1 & 0 & 0 \\ 0 & 0 & -1 \end{bmatrix} \tag{S6}$$

Then, the total transformation G between the coordinates is the matrix product:

$$G = T_4\, T_3(\psi)T_2(\theta)T_1(\phi) = \begin{bmatrix} sin\psi cos\theta & cos\psi cos\varphi + sin\psi sin\theta sin\varphi & sin\psi sin\theta cos\varphi - cos\psi sin\varphi \\ cos\psi cos\theta & -sin\psi cos\varphi + cos\psi sin\theta sin\varphi & sin\psi sin\varphi + cos\psi sin\theta cos\varphi \\ sin\theta & -cos\theta sin\varphi & cos\theta cos\varphi \end{bmatrix} \tag{S7}$$

In addition, offset corrections ($\varepsilon_\varphi, \varepsilon_\theta, \varepsilon_\psi$) are introduced here to correct for possible mounting misalignment in angle between the CG and the probe's tip. The values of these correction constants are determined via dedicated flight maneuvers (in Part C). Due to the offset in φ had an insignificant effect on the computed wind speed (Van Den Kroonenberg et al., 2008), therefore, ε_φ was not included in the calibration and was set to 0. Then, the three-rotation angle could be expressed as:

$$\begin{cases} \varphi = \varphi_i \\ \theta = \theta_i + \varepsilon_\theta \\ \psi = \psi_i + \varepsilon_\psi \end{cases} \tag{S8}$$

where φ_i, θ_i, and ε_ψ are the INS measured attitude angle.

The cross-product term ($\Omega_p \times R_p$) in Eq. (S2) describe the "lever arm" effect due to the tip of the 5HP not being placed at the CG of the UAV, and all are defined in earth coordinates. In the UAV, the displacement of the 5HP tip with respect to the CG of the UAV along the X-axis (L = 1.459 m) is larger than the displacement along the Y-axis (0 m), and Z-axis (0.173 m), so that the lateral and vertical separation distances can be negligible. Then, R_p can be expressed as:

$$R_p = G(t) \cdot \begin{bmatrix} L \\ 0 \\ 0 \end{bmatrix} = \begin{bmatrix} Lcos\psi cos\theta \\ Lsin\psi cos\theta \\ -Lsin\theta \end{bmatrix} \quad \text{(S9)}$$

Similarly, Ω_p can be expressed as:

$$\Omega_p = \begin{bmatrix} 0 \\ 0 \\ \dot{\psi} \end{bmatrix} + \begin{bmatrix} cos\psi & -sin\psi & 0 \\ sin\psi & cos\psi & 0 \\ 0 & 0 & 1 \end{bmatrix} \cdot \begin{bmatrix} 0 \\ \dot{\theta} \\ 0 \end{bmatrix} + \begin{bmatrix} cos\psi cos\theta & -sin\psi & cos\psi sin\theta \\ sin\psi cos\theta & cos\psi & sin\psi sin\theta \\ -sin\theta & 0 & cos\theta \end{bmatrix} \cdot \begin{bmatrix} \dot{\varphi} \\ 0 \\ 0 \end{bmatrix} = \begin{bmatrix} -\dot{\theta} sin\psi + \dot{\varphi} cos\psi cos\theta \\ \dot{\theta} cos\psi + \dot{\varphi} sin\psi cos\theta \\ \dot{\psi} - \dot{\varphi} sin\theta \end{bmatrix} \quad \text{(S10)}$$

Thus,

$$\Omega_p \times R_p = T_4 L \begin{bmatrix} -\dot{\theta} sin\theta cos\psi - \dot{\psi} sin\psi cos\theta \\ \dot{\psi} cos\psi cos\theta - \dot{\theta} sin\psi sin\theta \\ -\dot{\theta} cos\theta \end{bmatrix} \quad \text{(S11)}$$

Then, converting to a meteorological and inertial navigation frame of reference:

$$\Omega_p \times R_p = L \begin{bmatrix} \dot{\psi} cos\psi cos\theta - \dot{\theta} sin\psi sin\theta \\ -\dot{\theta} sin\theta cos\psi - \dot{\psi} sin\psi cos\theta \\ \dot{\theta} cos\theta \end{bmatrix} \quad \text{(S12)}$$

where $\dot{\psi}$ and $\dot{\theta}$ are the angular velocity of heading (ψ) and pitch (θ) angle. The air velocity component ($\widehat{U}_a$) with respect to the aircraft is measured by 5HP. In addition, wind measurements by aircraft are subject to flow distortion and needed to be corrected. According to Vellinga et al. (2013) and Crawford et al. (1996), considering the influence of lift-induced upwash, the wind components with respect to the aircraft ($\hat{u}_a, \hat{v}_a, \widehat{w}_a$), can be calculated as:

$$\widehat{U}_a = \begin{bmatrix} \hat{u}_a \\ \hat{v}_a \\ \widehat{w}_a \end{bmatrix} = \frac{|U_a|}{D} \begin{bmatrix} -1 \\ tan\beta \\ tan\alpha \end{bmatrix} + w_u \begin{bmatrix} sin\chi \\ 0 \\ -cos\chi \end{bmatrix} \quad \text{(S13)}$$

$$D = (1 + tan^2 \alpha + tan^2 \beta)^{1/2} \quad \text{(S14)}$$

where $|U_a|$ is the magnitude of the true airspeed, α is the angle of attack (the airstream with respect to the aircraft in the aircraft's vertical plane, with positive in the downward direction), β is the angle of sideslip (the angle of the airstream with respect to the aircraft in the aircraft's horizontal plane, with clockwise positive rotation), w_u is the vortex's tangential velocity experienced at the probe tip (i.e., lift-induced upwash), and χ is the vertical separation angle probe to wing (Vellinga et al., 2013). For UAV applications, the influence of flow distortion cans be ignored because the probe is long enough. For the measurement of true airspeed, the details of converting the pressures (static and dynamic) and total air temperature measured by the 5-hole probe (5HP) to the magnitude of the relative true airspeed were given in Sun et al. (2021). Lastly, integrating the equations above, the final geo-referenced wind vectors (u, v, w) are:

$$u = u_p - |U_a|D^{-1}[sin\psi cos\theta + tan\beta(cos\psi cos\phi + sin\psi sin\theta sin\phi) + tan\alpha(sin\psi sin\theta cos\phi - cos\psi sin\phi)] - L(\dot{\theta} sin\theta sin\psi - \dot{\psi} cos\psi cos\theta) \quad \text{(S15)}$$

$$v = v_p - |U_a|D^{-1}[cos\psi cos\theta - tan\beta(sin\psi cos\phi - cos\psi sin\theta sin\phi) + tan\alpha(cos\psi sin\theta cos\phi + sin\psi sin\phi)] - L(\dot{\psi} sin\psi cos\theta + \dot{\theta} cos\psi sin\theta) \quad \text{(S16)}$$

$$w = w_p - |U_a|D^{-1}[sin\theta - tan\beta cos\theta sin\phi - tan\alpha cos\theta cos\phi] + L\dot{\theta} cos\theta \quad \text{(S17)}$$

The last term on the right-hand of Eqs. (S15) to (S17) is the leverage effect correction term.

Former and the current (Section 3.1 in the main article) studies have shown that the influence of the leverage effect on the wind measurement could be neglected when the spatial separation (L) between the tip of the 5HP and the CG of the aircraft is small (e.g., less than 10 m) and the aircraft is not undergoing a pilot-induced pitching maneuver (Lenschow, 1986; Rautenberg et al., 2019). This simplification greatly reduced the complexity of geo-referenced wind vector calculation. For estimating the measurement precision (1σ) of the geo-reference wind vector from aircraft, Enriquez and Friehe (1995) gave the linearized Taylor series expansions of Eqs. (S15) to (S17) to determine the sensitivities of each of the geo-referenced wind velocity components with respect to each of the measured variables. By ignoring the leverage effect correction term and giving the assumptions of a negligible pitch angle (i.e., small-angle approximation), according to the equations derived by Enriquez and Friehe (1995), the 1σ uncertainty in the 3D wind vector due to the 1σ measurement error of the output physical quantity from the related sensor module can be approximated by:

$$\sigma_{u,U_a} \approx \sigma_{U_a} \sin\psi, \sigma_{u,\beta} \approx \sigma_\beta U_a \cos\psi, \sigma_{u,\psi} \approx \sigma_\psi U_a \cos\psi, \sigma_{u,u_p} \approx \sigma_{u_p} \quad \text{(S18)}$$

$$\sigma_{v,U_a} \approx \sigma_{U_a} \cos\psi, \sigma_{v,\beta} \approx \sigma_\beta U_a \sin\psi, \sigma_{v,\psi} \approx \sigma_\psi U_a \cos\psi, \sigma_{u,v_p} \approx \sigma_{v_p} \quad \text{(S19)}$$

$$\sigma_{w,\alpha} \approx \sigma_\alpha U_a, \sigma_{w,\theta} \approx \sigma_\theta U_a, \sigma_{w,w_p} \approx \sigma_{w_p} \quad \text{(S20)}$$

where σ_{u,U_a}, $\sigma_{u,\beta}$, $\sigma_{u,\psi}$, σ_{u,u_p}, σ_{v,U_a}, $\sigma_{v,\beta}$, $\sigma_{v,\psi}$, and σ_{u,v_p} represent the partial derivative of geo-reference horizontal wind component (u and v) with respect to U_a, β, ψ, and u_p or v_p. $\sigma_{w,\alpha}$, $\sigma_{w,\theta}$, and σ_{w,w_p} represent the partial derivative of geo-reference vertical wind (w) with respect to α, θ, and w_p. σ_{U_a}, σ_α, and σ_β are the measurement precision (1σ) of the directly measured variables U_a, α, and β from 5HP. σ_ψ, σ_θ, σ_{u_p}, σ_{v_p}, and σ_{w_p} are the measurement precision (1σ) of the attitude and velocity directly output by INS. Propagation of the contributions from each sensitivity item can give a good estimate of the overall measurement precision in computing the geo-referenced 3D wind vector (Garman et al., 2006). Eqs. (S18) to (S20) can then be combined to compute the overall measurement precision (1σ) in the geo-referenced 3D wind vector (σ_u, σ_v, σ_w):

$$\sigma_u = \sqrt{\sigma_{u,U_a}^2 + \sigma_{u,\beta}^2 + \sigma_{u,\psi}^2 + \sigma_{u,u_p}^2} \tag{S21}$$

$$\sigma_v = \sqrt{\sigma_{v,U_a}^2 + \sigma_{v,\beta}^2 + \sigma_{v,\psi}^2 + \sigma_{v,v_p}^2} \tag{S22}$$

$$\sigma_w = \sqrt{\sigma_{w,\alpha}^2 + \sigma_{w,\theta}^2 + \sigma_{w,w_p}^2} \tag{S23}$$

2 Part B: Calculation of the turbulent fluxes and their uncertainty

Calculation of the turbulent fluxes from aircraft follow the theory of conventional eddy covariance (EC) technique taking into account all the necessary corrections for open-path gas analyzer (Gioli et al., 2006; Aubinet et al., 2012). The main difference between airborne and ground-based EC is in the averaging approaches, that aircraft use spatial instead of time averaging to calculated the turbulent fluctuations of wind vertical component and associated scalars (Gioli et al., 2006; Crawford et al., 1996). As an example, the spatial average of vertical wind ($\overline{w}$) is defined as:

$$\overline{w} = \frac{1}{\overline{U_p}T} \sum_i w_i U_{p_i} \Delta t \tag{S24}$$

where $\overline{U_p}$ is the mean ground speed of the aircraft, U_{p_i} is the instantaneous ground speed, Δt is time increment, and T is the total time over the averaging space. Then, the geo-referenced wind components (u, v, w) are rotated using double rotation manner to force the average value of the lateral and the vertical wind components equals zero ($\bar{v} = 0$, $\overline{w} = 0$). Subsequently, turbulent fluxes are calculated and corrected for density effects due to heat and water vapor transfer [Webb-Pearman-Leuning (WPL) correction, Webb et al. (1980)]. The final equations for calculating the fluxes of sensible heat (H), latent heat (LE), and CO_2 after WPL correction can be expressed as:

$$H = \rho c_p \overline{w' T_a{}'} \tag{S25}$$

$$LE = \lambda(1 + \mu\sigma)\left(\overline{w'\rho_v'} + \frac{\overline{\rho_v}}{\overline{T}} \overline{w' T_a{}'}\right) \tag{S26}$$

$$F_C = \overline{w' \rho_C{}'} + \mu \frac{\overline{\rho_c}}{\overline{\rho_d}} \overline{w'\rho_v'} + (1 + \mu\sigma) \frac{\overline{\rho_c}}{\overline{T_a}} \overline{w' T_a{}'} \tag{S27}$$

where the overbar denotes the average value, the prime denotes fluctuations in variable about its average value; ρ, ρ_v, ρ_c, and ρ_d are the densities of air, water vapor, CO_2, and dry air, respectively; $\mu = m_a/m_v$ and $\sigma = \bar{\rho}_v/\bar{\rho}_d$; m_a and m_v are the molecular mass of dry and water vaper, respectively. T_a is the air temperature.

For assessment of the flux measurement error, the partial derivatives of Eqs. (S25) to (S27) with respect to their flux value derived by Liu et al. (2006) were used:

$$\frac{\sigma_H}{H} = \frac{\sigma_{\overline{w' T_a{}'}}}{\overline{w' T_a{}'}} \tag{S28}$$

$$\frac{\sigma_{LE}}{LE} = \left[\frac{\overline{w'\rho_v'}}{\overline{w' T_a{}'}} \frac{\sigma_{\overline{w'\rho'_v}}}{\overline{w'\rho_v'}} + \frac{\overline{\rho_v}}{\overline{T}} \frac{\sigma_{\overline{w' T_a{}'}}}{\overline{w' T_a{}'}}\right] \Big/ \left[\frac{\overline{w'\rho_v'}}{\overline{w' T_a{}'}} + \frac{\overline{\rho_v}}{\overline{T_a}}\right] \tag{S29}$$

$$\frac{\sigma_{Fc}}{Fc} = \frac{\overline{w'\rho_C'}}{Fc}\frac{\sigma_{\overline{w'\rho'_c}}}{\overline{w'\rho_C'}} + \frac{\mu\overline{w'\rho'_v}}{Fc}\frac{\overline{\rho_c}}{\overline{\rho_d}}\frac{\sigma_{\overline{w'\rho'_v}}}{\overline{w'\rho'_v}} + \frac{\overline{\rho_c}\,\overline{w'T_a'}(1+\mu\sigma)}{\overline{T}Fc}\frac{\sigma_{\overline{w'T_a'}}}{\overline{w'T_a'}} \qquad \text{(S30)}$$

The above expressions ignored the perturbations terms from the errors in the individual scalar (i.e., ρ_v, ρ_c, T) which were proved negligible small (Serrano-Ortiz et al., 2008). Then, these equations are used to estimate the impact of instrumental noise incurred in measurements of raw sensible heat, latent heat and CO_2 fluxes covariance on the final calculated fluxes (as propagated through the WPL terms).

3 Part C: Calibration results of the 'box' flight maneuver

In our calibration flight campaign, the first 'box' flight maneuver was used to correct the mounting misalignment in heading (ϵ_ψ) and pitch (ϵ_θ) angles between the 5HP and the CG of the UAV. The offset in roll angle (ε_φ) was not included in the calibration and was set to 0° since its influence on the wind calculation is minimal. The detailed procedure for acquiring the calibration parameter ϵ_ψ and ϵ_θ are given in Vellinga et al. (2013) and Sun et al. (2021). The calibration of the UAV-based EC system should occur in ideal atmospheric conditions, i.e., a constant mean horizontal wind component, near zero mean vertical wind. During the calibration, only the data from the straight sections of the 'box' flight maneuver were used. The calibration values ϵ_ψ and ϵ_θ were both determined iteratively until their values reached a steady state.

Before calibration, ϵ_ψ and ϵ_θ were set to their default value (0°). The offset ϵ_θ was first calibrated. The value of ϵ_θ was set to vary within the typical range of $\pm 1°$, and the mean vertical wind component ($\overline{w}$) was iteratively calculated using a step length of 0.2° to find the value of ϵ_θ for which $\overline{w}$ is zero. The individual straight sections of the 'box' maneuver are used. The results are shown in Figure S2. The average offset was calculated and served as the final value used in Eq. S8. The final iterative step resulted in an offset of -0.183° for ϵ_θ.

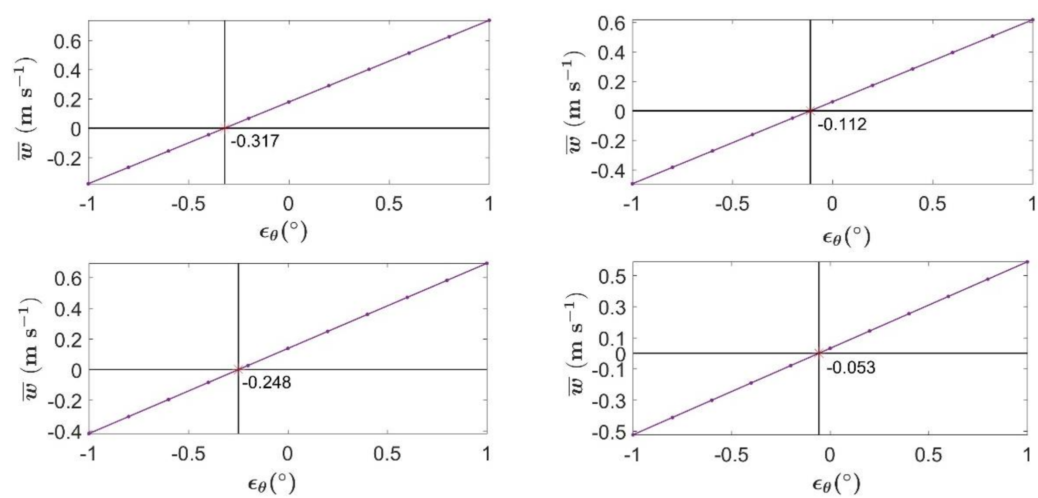

Figure S2. Offset values (ϵ_θ) in the pitch angle corresponding to the zero-averaged value of the vertical wind component ($\overline{w} = 0$). The final offset value (ϵ_θ) in the pitch angle was calculated by averaging the determined offset value from the individual straight sections of the 'box' maneuver.

Next, the offset ϵ_{ψ} was calibrated by setting the possible value to vary within the range between 0º and 4º and by iteratively calculating the horizontal wind speed using a step length of 0.5º. The final offset ϵ_{ψ} was determined from the straight sections of the 'box' maneuver by finding the minimum variances for horizontal wind direction ($\sigma_{U_{dir}}$) and wind speed velocity (σ_U). Figure S3 shows the results for ϵ_{ψ} from the final iterative session of the calibration. Figure S3b shows that $\sigma_{U_{dir}}$ and σ_U reach their minima at the offset value of 1.822º and 2.178º, respectively. The final offset value ϵ_{ψ} is determined as their average of 2º.

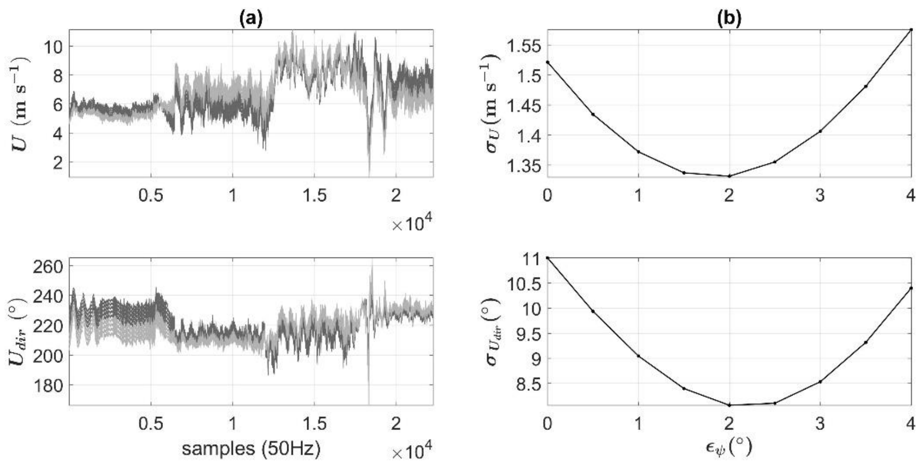

Figure S3. Offset values (ϵ_{θ}) in the pitch angle corresponding to the zero-averaged value of the vertical wind component ($\bar{w} = 0$). The final offset value (ϵ_{θ}) in the pitch angle was calculated by averaging the determined offset value from the individual straight sections of the 'box' maneuver.

References

Aubinet, M., Vesala, T., and Papale, D.: Eddy Covariance: A Practical Guide to Measurement and Data Analysis, Springer Atmospheric Sciences, Springer Netherlands, XXII, 438 pp., 10.1007/978-94-007-2351-1, 2012.

Crawford, T. L. and Dobosy, R. J.: A sensitive fast-response probe to measure turbulence and heat flux from any airplane, Boundary-Layer Meteorology, 59, 257-278, 10.1007/BF00119816, 1992.

Crawford, T. L., Dobosy, R. J., and Dumas, E. J.: Aircraft wind measurement considering lift-induced upwash, Boundary-Layer Meteorology, 80, 79-94, 10.1007/BF00119012, 1996.

Enriquez, A. G. and Friehe, C. A.: Effects of Wind Stress and Wind Stress Curl Variability on Coastal Upwelling, Journal of Physical Oceanography, 25, 1651-1671, https://doi.org/10.1175/1520-0485(1995)025<1651:EOWSAW>2.0.CO;2, 1995.

Garman, K. E., Hill, K. A., Wyss, P., Carlsen, M., Zimmerman, J. R., Stirm, B. H., Carney, T. Q., Santini, R., and Shepson, P. B.: An Airborne and Wind Tunnel Evaluation of a Wind Turbulence Measurement System for Aircraft-Based Flux Measurements, Journal of Atmospheric and Oceanic Technology, 23, 1696-1708, 10.1175/JTECH1940.1, 2006.

Gioli, B., Miglietta, F., Vaccari, F. P., and Zaldei, A.: The Sky Arrow ERA, an innovative airborne platform to monitor mass, momentum and energy exchange of ecosystems, Annals of Geophysics, 49, 109-116, 10.4401/ag-3159, 2006.

Khelif, D., Burns, S. P., and Friehe, C. A.: Improved Wind Measurements on Research Aircraft, Journal of Atmospheric and Oceanic Technology, 16, 860-875, 10.1175/1520-0426(1999)016<0860:IWMORA>2.0.CO;2, 1999.

Lenschow, D. H.: Aircraft Measurements in the Boundary Layer, in: Probing the Atmospheric Boundary Layer, edited by: Lenschow, D. H., American Meteorological Society, Boston, MA, Boston, https://doi.org/10.1007/978-1-944970-14-7_5, 1986.

Liu, H., Randerson, J. T., Lindfors, J., Massman, W. J., and Foken, T.: Consequences of Incomplete Surface Energy Balance Closure for CO2 Fluxes from Open-Path CO2/H2O Infrared Gas Analysers, Boundary-Layer Meteorology, 120, 65-85, 10.1007/s10546-005-9047-z, 2006.

Metzger, S., Junkermann, W., Butterbach-Bahl, K., Schmid, H. P., and Foken, T.: Measuring the 3-D wind vector with a weight-shift microlight aircraft, Atmos. Meas. Tech., 4, 1421-1444, 10.5194/amt-4-1421-2011, 2011.

Rautenberg, A., Allgeier, J., Jung, S., and Bange, J.: Calibration Procedure and Accuracy of Wind and Turbulence Measurements with Five-Hole Probes on Fixed-Wing Unmanned Aircraft in the Atmospheric Boundary Layer and Wind Turbine Wakes, Atmosphere, 10, 10.3390/atmos10030124, 2019.

Serrano-Ortiz, P., Kowalski, A. S., Domingo, F., Ruiz, B., and Alados-Arboledas, L.: Consequences of Uncertainties in CO2 Density for Estimating Net Ecosystem CO2 Exchange by Open-path Eddy Covariance, Boundary-Layer Meteorology, 126, 209-218, 10.1007/s10546-007-9234-1, 2008.

Sun, Y., Ma, J., Sude, B., Lin, X., Shang, H., Geng, B., Diao, Z., Du, J., and Quan, Z.: A UAV-Based Eddy Covariance System for Measurement of Mass and Energy Exchange of the Ecosystem: Preliminary Results, Sensors, 21, 10.3390/s21020403, 2021.

van den Kroonenberg, A., Martin, T., Buschmann, M., Bange, J., and Vörsmann, P.: Measuring the Wind Vector Using the Autonomous Mini Aerial Vehicle M2AV, Journal of Atmospheric and Oceanic Technology, 25, 1969-1982, 10.1175/2008JTECHA1114.1, 2008.

Vellinga, O. S., Dobosy, R. J., Dumas, E. J., Gioli, B., Elbers, J. A., and Hutjes, R. W. A.: Calibration and Quality Assurance of Flux Observations from a Small Research Aircraft*, Journal of Atmospheric and Oceanic Technology, 30, 161-181, 10.1175/JTECH-D-11-00138.1, 2013.

Webb, E. K., Pearman, G. I., and Leuning, R.: Correction of flux measurements for density effects due to heat and water vapour transfer, Quarterly Journal of the Royal Meteorological Society, 106, 85-100, https://doi.org/10.1002/qj.49710644707, 1980.

Williams, A. and Marcotte, D.: Wind Measurements on a Maneuvering Twin-Engine Turboprop Aircraft Accounting for Flow Distortion, Journal of Atmospheric and Oceanic Technology, 17, 795-810, 10.1175/1520-0426(2000)017<0795:WMOAMT>2.0.CO;2, 2000.